PROCEEDINGS OF SCIENCE

Model selection results from different BAO datasets – DE models and Ω_KCDM

Denitsa Staicova[a,*]

[a1] *Institute for Nuclear Research and Nuclear Energy, Bulgarian Academy of Sciences, Sofia, Bulgaria*

E-mail: dstaicova@inrne.bas.bg

The use of the baryonic acoustic oscillations (BAO) datasets offers a unique opportunity to connect the early universe and the late one. In this proceeding, we discuss recent results that used a marginalised likelihood to remove the $H_0 - r_d$ degeneracy and then tested it on different dark energy (DE) models. It was found that this approach which does not rely on calibration on r_d or H_0, allows us to obtain results, comparable to the ones calculated with standard likelihoods. Here we emphasize on the major differences that we observed for the two different BAO datasets that we employed – a transversal one, containing only angular BAO measurements, and a mixed one, containing both angular and radial BAO measurements. We see that the two datasets have different statistical preferences for DE models and also different preference for the curvature of the universe.

Corfu Summer Institute 2022 "School and Workshops on Elementary Particle Physics and Gravity",
28 August - 1 October, 2022
Corfu, Greece

*Speaker

PoS(CORFU2022)188

1. Introduction

The degeneracy between the Hubble parameter H_0 and the sound horizon horizon r_d is a known problem, sometimes called the $H_0 - r_d$ tension ([1, 2]). For the concordance ΛCDM cosmology, the sound horizon, which makes the baryonic acoustic oscillations (BAO) a standard ruler, is known and it depends on the ratio of baryonic to radiative content of the early universe. The problem, however, is that BAO measurements, both radial and transversal, always measure the quantity $H_0 r_d$. For this reason, in order to disentangle H_0 and r_d, it is required either a prior knowledge coming from the early universes (i.e a choice of r_d) [3], or a prior knowledge coming from the late universe (i.e. a prior on H_0) [4, 5]. In both cases, choosing a prior on either quantity will bring certain assumptions in our model, which will effectively lead to a calibration of the BAO measurement with either the early universe or the late one. While local measurements of H_0 [4, 5] are considered model-independent and are done with ever increasing precision, thanks to the newer instruments such as JWST [6] and the improvement of the methods, they are still at odds with the early universe measurements from the Planck mission [3]. The discrepancy between local universe and the early universe has been seen in different quantities - the Hubble constant H_0, the $\sigma_8 - S_8$ and other anomalies [2]. The tensions in cosmology have challenged our models for years now and have led to a lot of works looking for ways to resolve the problem or at least to mitigate it (for recent reviews, see [2, 7]).

In a series of articles [8–11], we considered the applications of different BAO datasets to constrain cosmological parameters and we looked for a way around the mentioned calibration leading to the $H_0 - r_d$ tension. Here we will discuss the approach in [10], in which we used a marginalisation procedure to integrate out of the likelihood χ^2 the factor $H_0 r_d$. This procedure allows us to completely avoid setting any prior on H_0 and r_d because our χ^2 no longer depends on them. Then, we use this uncalibrated by early or late universe likelihood, to perform full Bayesian analysis for different models of dark energy (DE). We find that without any other assumptions, the BAO datasets cannot constrain well the DE models, but by adding the type IA supernova dataset, the errors on the DE parameters become smaller. We also find that the two datasets we use have statistical preference for different cosmological models, which we will discuss in detail.

2. Constraining Dark Energy models

2.1 The equation of state of the Universe

We assume a Friedmann-Lemaître-Robertson-Walker metric, with a standard Friedman equation $(H(z)/H_0) = E(z)$ for :

$$E(z)^2 = \Omega_m(1+z)^3 + \Omega_K(1+z)^2 + \Omega_\Lambda(z), \tag{1}$$

where z is the redshift and the scale factor is $a = 1/(1+z)$, $H(z) := \dot{a}/a$ is the Hubble parameter at redshift z and H_0 is the Hubble parameter today. Ω_m, Ω_Λ, and Ω_K are the fractional densities of matter, DE, and the spatial curvature at redshift $z = 0$.

We consider two types of dark energy models. First, we consider an expansion of ΛCDM in the form of the Chevallier-Polanski-Linder parametrization (CPL) ([12–15]) of the $wwaCDM$ model:

$$\Omega_\Lambda(z) = \Omega_\Lambda^{(0)} \exp\left[\int_0^z \frac{3(1+w(z'))dz'}{1+z'}\right] \tag{2}$$

in which we considered three possible models:

$$w(z) = \begin{cases} w_0 + w_a z & \text{Linear} \\ w_0 + w_a \frac{z}{z+1} & \text{CPL} \\ w_0 - w_a \log(z+1) & \text{Log} \end{cases}, \tag{3}$$

which recover the ΛCDM for $w_0 = -1, w_a = 0$.

As an alternative to ΛCDM, we consider the phenomenologically Emergent Dark Energy (pEDE) model [16, 17] and its generalization (gEDE). gEDE is described by:

$$\Omega_{DE}(z) = \Omega_\Lambda \frac{1 - \tanh(\bar{\Delta}\log_{10}(\frac{1+z}{1+z_t}))}{1 + \tanh(\bar{\Delta}\log_{10}(1+z_t)}, \tag{4}$$

with pEDE-CDM recovered for $\bar{\Delta} = 1$, and ΛCDM for $\bar{\Delta} = 0$. Here, the transitional redshift z_t is found from $\Omega_{DE}(z_t) = \Omega_m(1+z_t)^3$, see [17].

The radial BAO projection $D_H(z) = c/H(z)$ is found from:

$$\frac{D_H}{r_d} = \frac{c}{H_0 r_d}\frac{1}{E(z)}. \tag{5}$$

The tangential BAO measurements expressed in terms of the angular diameter distance D_A/r_d are:

$$\frac{D_A}{r_d} = \frac{c}{H_0 r_d} f(z), \tag{6a}$$

where:

$$f(z) = \frac{1}{(1+z)\sqrt{|\Omega_K|}}\mathrm{sinn}\left[|\Omega_K|^{1/2}\Gamma(z)\right]. \tag{6b}$$

The BAO angular scale measurement $\theta_{BAO}(z)$ needed for the θ_{BAO} dataset is :

$$\theta_{BAO}(z) = \frac{r_d}{(1+z)\,D_A(z)} = \frac{H_0 r_d}{c} h(z), \tag{7}$$

with:

$$h(z) = \frac{1}{(1+z)f(z)} \tag{8}$$

The SNIa measurements are described by their distance modulus which is related to the luminosity distance ($D_A = d_L(z)/(1+z)^2$) through:

$$\mu_B(z) - M_B = 5\log_{10}[d_L(z)] + 25\,, \tag{9}$$

where d_L is measured in units of Mpc, and M_B is the absolute magnitude.

2.2 The χ^2 redefinition

For the BAO points, we redefine χ^2 in a way that isolates $\frac{c}{H_0 r_d}$, i.e. we perform a maginalization procedure[18–21]. Omitting the details that can be found in [10], the final χ^2 becomes:

$$\tilde{\chi}^2_{BAO} = C - \frac{B^2}{A} + \log\left(\frac{A}{2\pi}\right). \tag{10}$$

where:

$$A = f^j(z_i) C_{ij} f^i(z_i), \tag{11a}$$

$$B = \frac{f^j(z_i) C_{ij} v^i_{model}(z_i) + v^j_{model}(z_i) C_{ij} f^i(z_i)}{2}, \tag{11b}$$

$$C = v^{model}_j C_{ij} v^{model}_i. \tag{11c}$$

Here $\vec{v}_{obs}$ is the vector of the observed points at each z (i.e., D_M/r_d, D_H/r_d, D_A/r_d or θ_{BAO}) and $\vec{v}_{model}$ is the theoretical prediction of the model. C_{ij} is the covariance matrix (for uncorrelated points, it becomes a diagonal matrix with elements equal to the inverse errors σ_i^{-2}.

For the θ_{BAO} data, the χ^2 has the same form, but the coefficients are as follows:

$$A_\theta = \sum_{i=1}^{N} \frac{h(z_i)^2}{\sigma_i^2}, \tag{12a}$$

$$B_\theta = \sum_{i=1}^{N} \frac{\theta^i_D \, h(z_i)}{\sigma_i^2}, \tag{12b}$$

$$C_\theta = \sum_{i=1}^{N} \frac{\left(\theta^i_D\right)^2}{\sigma_i^2}. \tag{12c}$$

For the SN data, we assumed no prior constraint on M_B, and we integrated the probabilities over M_B and H_0 [18, 22–24] to get the marginalized χ^2:

$$\tilde{\chi}^2_{SN} = D - \frac{E^2}{F} + \ln\frac{F}{2\pi}, \tag{13}$$

where:

$$D = \sum_i \left(\Delta\mu \, C^{-1}_{cov} \, \Delta\mu^T\right)^2, \tag{14a}$$

$$E = \sum_i \left(\Delta\mu \, C^{-1}_{cov} \, E\right), \tag{14b}$$

$$F = \sum_i C^{-1}_{cov}, \tag{14c}$$

where $\Delta\mu = \mu^i - 5\log_{10}\left[d_L(z_i)\right)$, E is the unit matrix, and C^{-1}_{cov} is the inverse covariance matrix of the dataset [25].

2.3 Datasets and methods

We use two different BAO datasets, to which we add the binned Pantheon supernovae dataset with its covariance matrix. The BAO datasets can be found summarized in [10]. First, we use a BAO dataset, denoted as BAO, which contains various angular data-points combined with few points from the most recent to date eBOSS data release (DR16), which come as angular (D_M) and radial (D_H) measurements and their covariance. The second dataset is denoted as BAO_θ and it consists of 15 transversal BAO measurements used for clustering analysis [26]. These points have the advantage that they are uncorrelated and that they do not assume a fiducial cosmology, particularly on the Ω_K parameter, which is included in the standard BAO analysis [26]. To the BAO points, we add the binned Pantheon dataset, which contains 40 supernovae luminosity measurements in the redshift range $z \in (0.01, 2.3)$ [27] (called here "SN").

The priors we used can be found in [10]. We use the MCMC nested sampler, implemented in the open-source package *Polychord* [28] with the *GetDist* package [29] to present the results.

2.4 Results

After performing the MCMC, the results we obtained can be summarized as follows. The BAO-only datasets do not constrain the DE models parameters, particularly the parameter w_a is practically unconstrained and w_0 is found with a big error. The only parameter that gets a good constraint is Ω_m. The combined BAO + SN dataset reduces the errors significantly and allows to put better constraints on w_0 but again, it does not constrain well w_a. The results we get for the DE models for the combined datasets are in the table below:

Model	w_0	w_a
BAO +SN		
wCDM	-0.99 ± 0.05	
wwaCDM	-1.18 ± 0.14	-0.38 ± 0.67
$BAO_\theta + SN$		
wCDM	-1.08 ± 0.14	
wwaCDM	-1.09 ± 0.09	-0.31 ± 0.74

This result is consistent with the SDSS-IV results [30], which obtains: $w_0 = -0.939 \pm 0.073$, $w_a = -0.31 \pm 0.3$ for the combination BAO+SN+CMB, but $w_0 = -0.69 \pm 0.15$ when only the BAO dataset is used. We see that our result is comparable to this, even though some precision is lost due to the marginalization procedure.

A very interesting result we obtained is that the two BAO datasets do not prefer the same DE models. This becomes very obvious when one uses statistical measures to compare the DE models we consider to the ΛCDM model. In [10] we use 4 different measures: the Akaike information criterion (AIC), the Bayesian information criterion (BIC), the deviance information criterion (DIC), and the Bayes factor (BF) [31]. The AIC and BIC favor systematically the ΛCDM model as the model with the least number of parameters, with the only exclusion being the pEDE model. For this reason, in this work, we present only the other two measures DIC and BF.

The DIC estimator is defined as:

$$\mathrm{DIC} = 2\overline{(D(\theta))} - D(\bar{\theta}), \tag{15}$$

where θ is the vector of parameters being varied in the model, the overline denotes the usual mean value, and $D(\theta) = -2\ln(\mathcal{L}(\theta)) + C$, where C is a constant. With this definition, we calculate the difference $\Delta\text{DIC}_{\text{model}} = \text{DIC}_{\Lambda\text{CDM}} - \text{DIC}_{\text{model}}$. A positive ΔDIC points to a preference toward the DE model, negative – toward ΛCDM with $|\Delta\text{DIC}| \geq 2$ signifying a possible tension.

The Bayes factor is defined as:

$$B_{ij} = \frac{p(d|M_i)}{p(d|M_j)},$$

where $p(d|M_i)$ is the Bayesian evidence for model M_i, which we calculate numerically with Polychord. We use the $ln(B_{0i})$, where "0" is ΛCDM, which we compare with all the other models (denoted by the index "i") . According to the Jeffry's scale, $ln(B_{ij}) < 1$ is inconclusive for any of the models, for 1-2.5 one finds weak support for the model "i" and above 2.5, there is moderate and strong support for the model "i". A minus sign gives the same for model "j" [32].

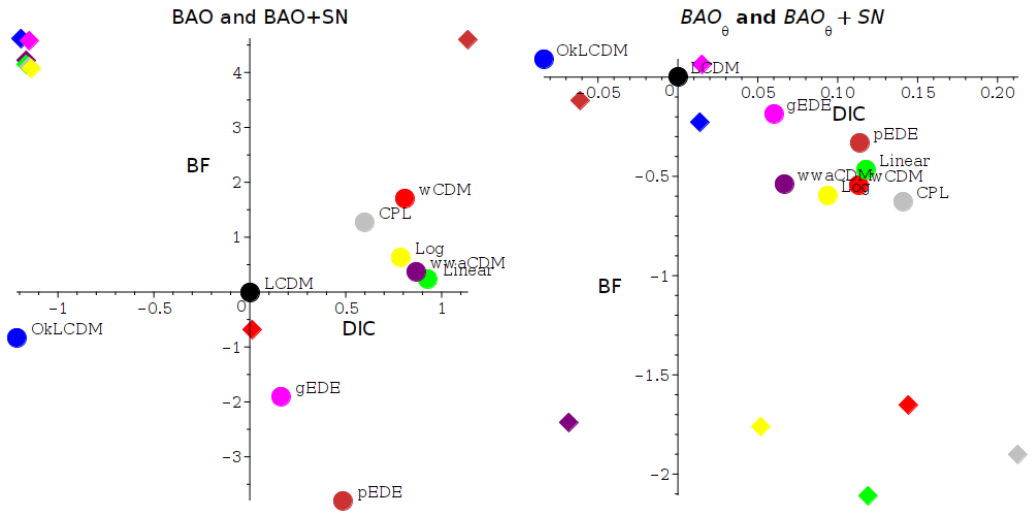

Figure 1: *The DIC-BF plane for the BAO and BAO + SN points (left) and BAO_θ and BAO_θ + SN points (right). We present everywhere the BAO only points with solid spheres, the BAO+SN points with diamonds.*

The results from Table 3 and 4 in [10] are presented on Fig. 1, where the solid circle signifies the BAO dataset and the diamond, the BAO + SN datset. On the left figure, the values of the BAO + SN points are divided by 4 in both directions to fit the plot. In order for a model to be better than ΛCDM in DIC, it has to be in the right side of the plot, in order for it to be better with respect to BF, it has to be in the lower part of the plot. So the best models to challenge ΛCDM are the ones in the lower right corner of the plots. We see that for the BAO points, these models are only pEDE and gEDE. For the BAO+SN points, there is no such model except maybe for wCDM. On the other hand, the $BA0_\theta$ points exhibit a totally different behavior. We see that there are a lot of comparable to ΛCDM model for the BAO_θ alone points, but there are also such points for the BAO_θ + SN - basically all of the CPL models are in the right part of the plot, even though with respect to DIC, the distance is very small, meaning a not significant preference for DE models. The BF value, however, signifies some tension with ΛCDM. One can see that this dataset seems to be much more favorable to the different DE models from statistical point of view. The errors for both datasets are comparable. Such results have also been found in other model-independent approaches [33, 34].

Another important difference between the two BAO datasets can be seen is in the Ω_KCDM model. From our results presented in [10] we see that the$BAO+SN$ dataset prefers a closed universe ($\Omega_K = -0.21 \pm 0.07$), while the $BAO_\theta + SN$ dataset prefers a flat one ($\Omega_K = -0.09 \pm 0.15$). Such strong deviation from the flat universe seems questionable, and because of this, we investigate it further below. We study the dependency of the results on the prior on Ω_K using two priors – the standard one $\Omega_K \in [-0.3, 0.3]$ and a "large" one – $\Omega_K \in [-0.7, 3]$. One can see the results of the different priors on Fig. 2. The full posteriors are in the Appendix.

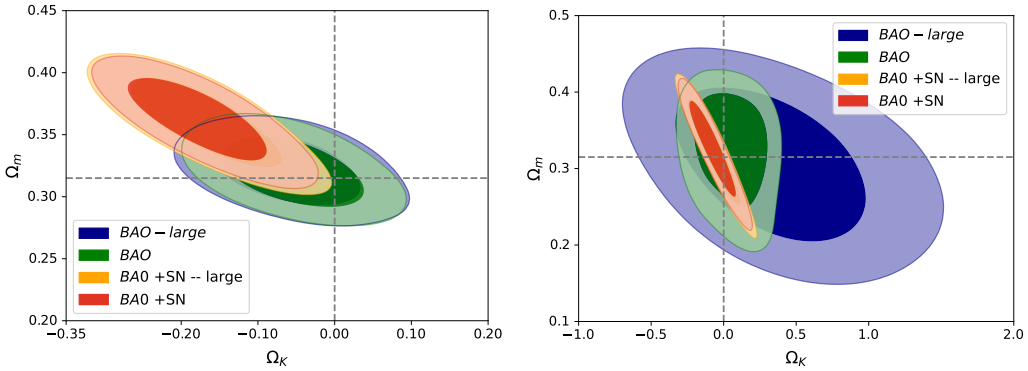

Figure 2: *Posterior distribution for Ω_m and Ω_K for BAO and BAO_θ datasets to the left and right, respectively*

From the figure, one can see that there is a significant difference with respect to the constraints on Ω_K and Ω_m for the two datasets. The BAO_θ points, with and without the addition of the SN points are centered around 0 and the BAO_θ points alone basically do not constrain Ω_K at all. Notably, in the negative direction, there is a problem with the integration, thus the prior is smaller, so the best constraint we find is $|\Omega_K| < 1$. For the BAO points, on the other hand, we see that the mean value is centered at negative Ω_K and adding the SN points do not help. One can consider two possible explanations of this result. Either it is due to the fact that we lose sensitivity to the Ω_K parameter in this marginalised form of the χ^2, especially for the SN points. Or this is a result of the specific processing of the BAO_θ dataset that cleaned up any fiducial cosmology, particularly with respect to the spatial curvature, rendering it insensitive to this parameter. Or maybe we are seeing both effects simultaneously, with the marginalisation removing an important leverage on the value of Ω_K. Note, on the figure we have denoted the flat cosmology with a line and also, the Planck matter density Ω_m. One can see that in the BAO+SN case, the negative curvature is achieved on the price of higher Ω_m, which leads also to higher Ω_Λ, since due to the marginalization procedure, there is no other parameter to compensate for the non-zero Ω_K.

The discussion on the value of Ω_K is not new [2, 35–38]. Recently, [39] studied different DE cosmologies and found that there are indications of negative Ω_K in most of them. An interesting study from the point of view of renormalization group approach argues that the flat universe is the only one offering scale-free, non-singular background for cosmological perturbations[40]. From the literature we see that while the deviation from the flat universe is usually small, model-independent approaches seem to give larger deviations, similar to the ones we obtained, for example [35, 41, 42]. Also while strange that adding the SN data leads to bigger Ω_K, it can be seen also in [39] where CMB+BAO has bigger Ω_K than CMB+Pantheon. The Planck data alone also seem to prefer a

closed universe [3].

2.5 Discussion

We have summarized our results on the use of a χ^2 marginalization procedure on a BAO + SN datasets that we utilized to study different DE modes. The results on the DE models are very similar to the already published in the literature, which shows that our procedure can be useful for studying alternatives to the ΛCDM model. On the other hand, it also allowed us to study the difference between the two BAO datasets that we chose to investigate – an angular one that is claimed to be cleaned up from the fiducial cosmology (BAO_θ) and a mixed radial and angular (BAO). One can see that in terms of DE models, the BAO_θ dataset leads to significantly less preference for ΛCDM which we demonstrate with the help of different statistical measures comparing the models. In terms of Ω_KCDM, the two sets of points also possess different behavior, with BAO_θ preferring a flat universe, while BAO alone having a strong preference for a closed one. We cannot tell to what extend the latter is a numerical artifact due to the fact we marginalize over $H_0 r_d$, which may make it much less numerically sensitive to the curvature of the universe. On the other hand, this approach may offer a way to study how measurements processing affects their bias towards certain models and to allow for a better comparison between different datasets.

Acknowledgments

D.S. is thankful to Bulgarian National Science Fund for support via research grant KP-06-N38/11

References

[1] L. Knox and M. Millea, *Hubble constant hunter's guide*, *Phys. Rev. D* **101** (2020) 043533 [1908.03663].

[2] E. Abdalla et al., *Cosmology intertwined: A review of the particle physics, astrophysics, and cosmology associated with the cosmological tensions and anomalies*, *JHEAp* **34** (2022) 49 [2203.06142].

[3] Planck collaboration, *Planck 2018 results. VI. Cosmological parameters*, *Astron. Astrophys.* **641** (2020) A6 [1807.06209].

[4] A.G. Riess et al., *A Comprehensive Measurement of the Local Value of the Hubble Constant with 1 km s^{-1} Mpc^{-1} Uncertainty from the Hubble Space Telescope and the SH0ES Team*, *Astrophys. J. Lett.* **934** (2022) L7 [2112.04510].

[5] A.G. Riess, L. Breuval, W. Yuan, S. Casertano, L.M. ~Macri, D. Scolnic et al., *Cluster Cepheids with High Precision Gaia Parallaxes, Low Zeropoint Uncertainties, and Hubble Space Telescope Photometry*, 2208.01045.

[6] W. Yuan, A.G. Riess, S. Casertano and L.M. Macri, *A First Look at Cepheids in a Type Ia Supernova Host with JWST*, *Astrophys. J. Lett.* **940** (2022) L17 [2209.09101].

[7] V. Poulin, T.L. Smith and T. Karwal, *The Ups and Downs of Early Dark Energy solutions to the Hubble tension: a review of models, hints and constraints circa 2023*, 2302.09032.

[8] D. Benisty and D. Staicova, *Testing late-time cosmic acceleration with uncorrelated baryon acoustic oscillation dataset*, *Astron. Astrophys.* **647** (2021) A38 [2009.10701].

[9] D. Benisty, J. Mifsud, J.L. Said and D. Staicova, *On the Robustness of the Constancy of the Supernova Absolute Magnitude: Non-parametric Reconstruction & Bayesian approaches*, 2202.04677.

[10] D. Staicova and D. Benisty, *Constraining the dark energy models using Baryon Acoustic Oscillations: An approach independent of $H_0 \cdot r_d$*, 2107.14129.

[11] D. Staicova, *DE Models with Combined $H_0 \cdot r_d$ from BAO and CMB Dataset and Friends*, *Universe* **8** (2022) 631 [2211.08139].

[12] M. Chevallier and D. Polarski, *Accelerating universes with scaling dark matter*, *Int. J. Mod. Phys. D* **10** (2001) 213 [gr-qc/0009008].

[13] E.V. Linder, *Exploring the expansion history of the universe*, *Phys. Rev. Lett.* **90** (2003) 091301 [astro-ph/0208512].

[14] E.V. Linder and D. Huterer, *How many dark energy parameters?*, *Phys. Rev. D* **72** (2005) 043509 [astro-ph/0505330].

[15] V. Barger, E. Guarnaccia and D. Marfatia, *Classification of dark energy models in the (w(0), w(a)) plane*, *Phys. Lett. B* **635** (2006) 61 [hep-ph/0512320].

[16] X. Li and A. Shafieloo, *A Simple Phenomenological Emergent Dark Energy Model can Resolve the Hubble Tension*, *Astrophys. J. Lett.* **883** (2019) L3 [1906.08275].

[17] X. Li and A. Shafieloo, *Evidence for Emergent Dark Energy*, *Astrophys. J.* **902** (2020) 58 [2001.05103].

[18] R. Lazkoz, S. Nesseris and L. Perivolaropoulos, *Exploring Cosmological Expansion Parametrizations with the Gold SnIa Dataset*, *JCAP* **11** (2005) 010 [astro-ph/0503230].

[19] S. Basilakos and S. Nesseris, *Testing Einstein's gravity and dark energy with growth of matter perturbations: Indications for new physics?*, *Phys. Rev. D* **94** (2016) 123525 [1610.00160].

[20] F.K. Anagnostopoulos and S. Basilakos, *Constraining the dark energy models with $H(z)$ data: An approach independent of H_0*, *Phys. Rev. D* **97** (2018) 063503 [1709.02356].

[21] D. Camarena and V. Marra, *On the use of the local prior on the absolute magnitude of Type Ia supernovae in cosmological inference*, *Mon. Not. Roy. Astron. Soc.* **504** (2021) 5164 [2101.08641].

[22] E. Di Pietro and J.-F. Claeskens, *Future supernovae data and quintessence models*, *Mon. Not. Roy. Astron. Soc.* **341** (2003) 1299 [astro-ph/0207332].

PoS(CORFU2022)188

[23] S. Nesseris and L. Perivolaropoulos, *A Comparison of cosmological models using recent supernova data*, *Phys. Rev. D* **70** (2004) 043531 [astro-ph/0401556].

[24] L. Perivolaropoulos, *Constraints on linear negative potentials in quintessence and phantom models from recent supernova data*, *Phys. Rev. D* **71** (2005) 063503 [astro-ph/0412308].

[25] H.-K. Deng and H. Wei, *Null signal for the cosmic anisotropy in the Pantheon supernovae data*, *Eur. Phys. J. C* **78** (2018) 755 [1806.02773].

[26] R.C. Nunes, S.K. Yadav, J.F. Jesus and A. Bernui, *Cosmological parameter analyses using transversal BAO data*, *Mon. Not. Roy. Astron. Soc.* **497** (2020) 2133 [2002.09293].

[27] Pan-STARRS1 collaboration, *The Complete Light-curve Sample of Spectroscopically Confirmed SNe Ia from Pan-STARRS1 and Cosmological Constraints from the Combined Pantheon Sample*, *Astrophys. J.* **859** (2018) 101 [1710.00845].

[28] W.J. Handley, M.P. Hobson and A.N. Lasenby, *PolyChord: nested sampling for cosmology*, *Mon. Not. Roy. Astron. Soc.* **450** (2015) L61 [1502.01856].

[29] A. Lewis, *GetDist: a Python package for analysing Monte Carlo samples*, 1910.13970.

[30] eBOSS collaboration, *Completed SDSS-IV extended Baryon Oscillation Spectroscopic Survey: Cosmological implications from two decades of spectroscopic surveys at the Apache Point Observatory*, *Phys. Rev. D* **103** (2021) 083533 [2007.08991].

[31] A.R. Liddle, *Information criteria for astrophysical model selection*, *Mon. Not. Roy. Astron. Soc.* **377** (2007) L74 [astro-ph/0701113].

[32] H. Jeffreys, *The Theory of Probability*, Oxford Classic Texts in the Physical Sciences (1939).

[33] R.C. Bernardo, D. Grandón, J. Levi Said and V.H. Cárdenas, *Dark energy by natural evolution: Constraining dark energy using Approximate Bayesian Computation*, 2211.05482.

[34] A. Mehrabi and J. Levi Said, *Gaussian discriminators between ΛCDM and wCDM cosmologies using expansion data*, *Eur. Phys. J. C* **82** (2022) 806 [2203.01817].

[35] J. Ryan, S. Doshi and B. Ratra, *Constraints on dark energy dynamics and spatial curvature from Hubble parameter and baryon acoustic oscillation data*, *Mon. Not. Roy. Astron. Soc.* **480** (2018) 759 [1805.06408].

[36] S. Vagnozzi, A. Loeb and M. Moresco, *Eppur è piatto? The Cosmic Chronometers Take on Spatial Curvature and Cosmic Concordance*, *Astrophys. J.* **908** (2021) 84 [2011.11645].

[37] E. Di Valentino, A. Melchiorri and J. Silk, *Planck evidence for a closed Universe and a possible crisis for cosmology*, *Nature Astron.* **4** (2019) 196 [1911.02087].

[38] S. Vagnozzi, E. Di Valentino, S. Gariazzo, A. Melchiorri, O. Mena and J. Silk, *The galaxy power spectrum take on spatial curvature and cosmic concordance*, *Phys. Dark Univ.* **33** (2021) 100851 [2010.02230].

[39] W. Yang, W. Giarè, S. Pan, E. Di Valentino, A. Melchiorri and J. Silk, *Revealing the effects of curvature on the cosmological models*, *Phys. Rev. D* **107** (2023) 063509 [2210.09865].

[40] R. Jimenez, A.R. Khalife, D.F. Litim, S. Matarrese and B.D. Wandelt, *Why is zero spatial curvature special?*, 2210.10102.

[41] J.-J. Wei and X.-F. Wu, *An Improved Method to Measure the Cosmic Curvature*, *Astrophys. J.* **838** (2017) 160 [1611.00904].

[42] J. Stevens, H. Khoraminezhad and S. Saito, *Constraining the spatial curvature with cosmic expansion history in a cosmological model with a non-standard sound horizon*, 2212.09804.

A. Appendix

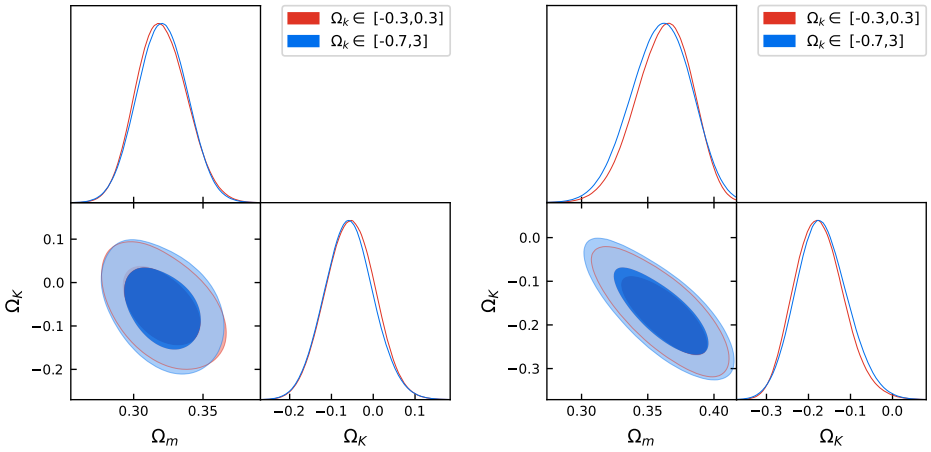

Figure 3: *Posterior distribution for Ω_m and Ω_K for BAO (left panel) and BAO+SN (right panel) datasets*

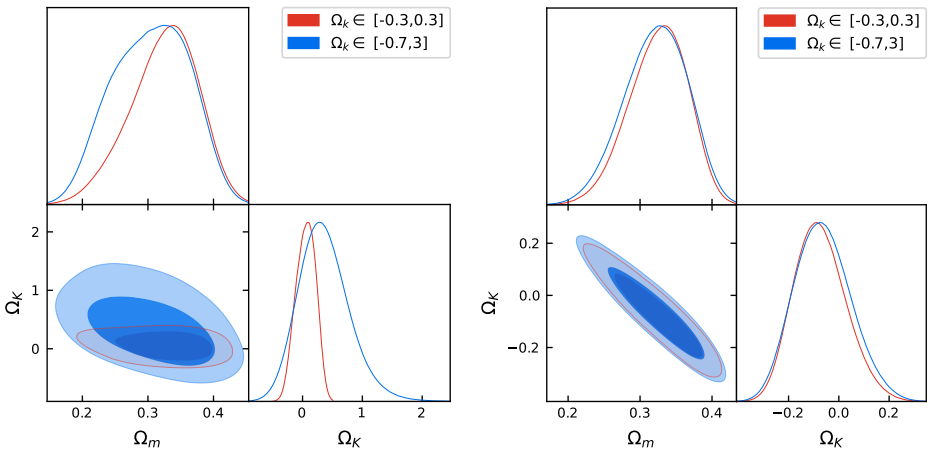

Figure 4: *Posterior distribution for Ω_m and Ω_K for BAO$_\theta$ (left) and BAO$_\theta$+SN (right) datasets*